

DEVELOPMENT OF A NOVEL ICE OIL BOOM FOR FLOWING WATERS

Gee Tsang

National Water Research Institute
Canada Centre for Inland Waters
Environment Canada
Burlington, Ontario, Canada

Nick Vanderkooy

Environmental Emergency Branch
Environmental Protection Service
Environment Canada
Toronto, Ontario, Canada

ABSTRACT: To contain and recover oil in an ice-infested river, an ice-free area has to be created wherein conventional clean-up gear may be employed. A joint Canada-United States study was begun to develop a barrier which would allow the oil to pass through while barring ice floes from entering the recovery site area. Theoretical and laboratory study showed that the ice floes could be deflected successfully from an oil spill recovery site. The U.S. Coast Guard financed the construction of the prototype and it was successfully tested at the Canadian Coast Guard Base in the Detroit River, Amherstburg, Ontario.

The ice boom utilizes the ruddering principle, used by glance booms for the lumber industry. It consists of a sturdy body and a number of short fins or rudders. The angle between the boom and the fins is variable. The upstream end of the boom is tied to the shore. When the fins are gradually closed from the initially open position, the force of the current on the fins brings the boom gradually into the flow. The out-swing boom then prevents the ice floes from entering the area behind it and thus creates the desirable ice-free area. Openings are provided in the boom for the oil slick to pass through. After the oil passes through the boom, it may be contained and recovered by conventional methods.

Field experiments showed that deployment and manipulation of the boom could be carried out readily. It was also apparent that the fins created a surface current deflecting the oil slick directly toward the shore. Quantitative design criteria have been obtained.

Background

In rivers with drifting ice floes, conventional oil booms placed in the current will be ripped apart and oil spill recovery devices jammed. The operation of small craft also will be hazardous. Ice floes are common in rivers during the winter months, as is the case, for example, in the Detroit and St. Clair rivers.¹

The problem of how to deal with oil spills under the above conditions was identified by the joint Canada-U.S. study—Operation Preparedness—which was carried out under the auspices of the "Joint Canada-United States Marine Pollution Contingency Plan". Participating agencies were from both federal governments, the state of Michigan, the Province of Ontario, the Lambton Industrial Society, and the Walpole Island Indian Reserve.

To contain and recover oil in an ice-infested river, an ice-free area has to be created first, in which conventional cleanup gear may be employed. Such an area is obtained if a barrier can be set up which, while permitting the oil slick to pass through, will bar ice floes from entering the area. Tsang² proposed the use of perforated booms at an

angle to the flow. While the slick should have little difficulty in passing through the openings provided, in the boom, the ice floes would be guided by the boom and deflected to one side.

It is difficult to contain oil by conventional booms, even under ice-free conditions, on fast flowing water.^{3,4} Also, their deployment is difficult because they need to be anchored at two or more points. If an ice boom is to be developed, therefore, it is desirable that it divert the oil to the slow shore region for containment and recovery and that it can be deployed from the shore only.

Glance booms have long been used by the pulp and paper industry to confine pulp wood to the desired channel. Figure 1 shows the configuration of a glance boom. Such a boom needs only to be moored by its upstream end from the shore. The fins or rudders, when impinged on by the flow, will take the boom into the current. By varying the angle between the fins and the boom, the angle between the boom and the current can be changed. The oncoming pulp wood, upon meeting the boom, is guided to one side.

An ice infested river is similar to a river transporting pulp wood. A glance boom, therefore, may be used as an ice barrier. If perforations are provided in the boom, then the oil slick will be able to flow through them to the ice-free area behind. The surface current, after flowing through the openings, will impinge on the fins and be deflected toward the shore, carrying the oil with it.

Such a boom also has a very desirable built-in stress-relief characteristic: should it be hit by an extraordinarily large ice floe, it will simply yield by swinging toward the shore instead of failing. Once the ice floe passes, the boom will swing back into the current again.

It is worth mentioning that the glance boom also inspired the development of boom deflectors by Brodsky *et al.*⁵ The deflectors are in the form of individual fins that can be clipped onto conventional booms. The clipping of deflectors to a boom makes the boom a straight deflection boom that only needs to be moored by its upstream end. Upon meeting the boom, an oil slick is guided to the desirable point for recovery.

Deflecting the oil slick toward the shore region by deflection of the surface current also has been contemplated by Eryuzlu and Hausser.⁶ A model study of the deflectors, simulating the St. Lawrence River situation, showed that several meters of the surface layer should be deflected. This calls for the construction of massive deflectors and mooring structures.

Theory

The glance booms as shown in Figure 1 are linked together either with ropes or shackles. Both laboratory and field tests showed that

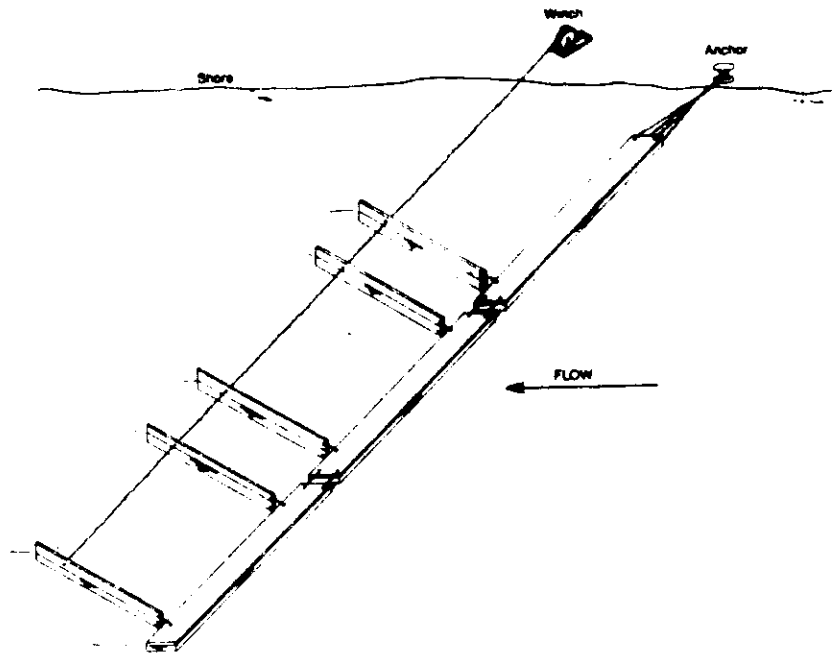
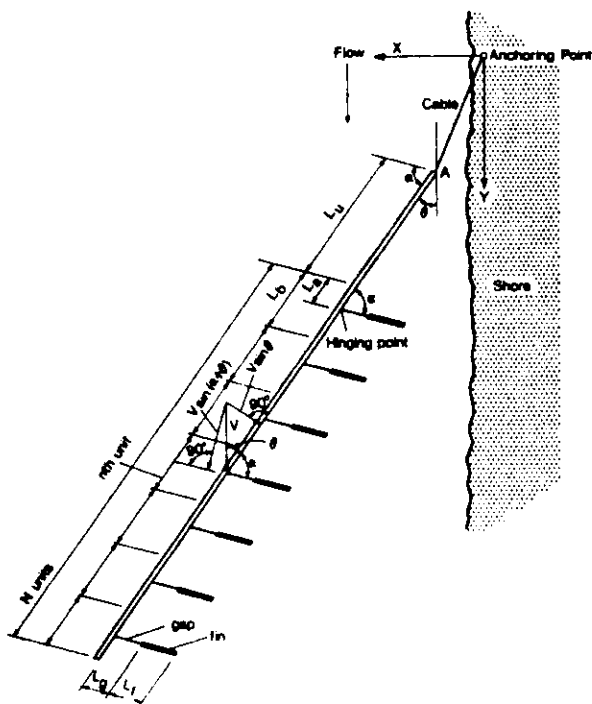


Figure 1. Glance boom used by timber industry

such flexible booms deform excessively when hit by large ice floes. The ice-oil boom to be developed, therefore, should be rigidly connected between units.

Figure 2 shows a rigidly constructed boom of N units. Each unit comprises a section of the boom body of length L_b and a fin of length L_f . The fin is hinged to the boom section at a distance L_a from the upstream end of the section and L_h is the distance between the fin and the centerline of the boom. L_a is for reducing the turbulence behind the boom. The diagram shows that when the angle between the fin and the boom is α , the equilibrium angle between the boom and the flow is θ . The upstream unfinned part is for protecting the fins from ice damage. Detailed analysis was made for such a boom,¹ and is summarized below.



It can be seen from Figure 2 that the current exerts a drag on the boom body itself, including the upstream protective part. This drag results in a counterclockwise moment about the upstream end of the boom point A. Also, drags are produced on the fins and they produce a clockwise moment about point A. In nondimensional forms, these moments are given by

$$M_b = 3\pi^2 \theta \left[\frac{L_b}{L_a} \left(\frac{1}{2} \frac{L_b}{L_a} + N \right) + \frac{N^2}{2} \right] \quad (1)$$

$$M_f = 3\pi^2 (\alpha + \theta) \frac{A_f}{A_b} N \left[\left(\frac{L_b}{L_a} + \frac{L_b}{L_a} + \frac{N-1}{2} \right) \cos \alpha - \left(\frac{L_b}{L_a} + \frac{L_f}{2L_a} \right) \right] \quad (2)$$

where the subscripts b and f refer to the boom and the fins respectively. The multiplying of M_b and M_f by $(C_D \rho V^2 A_b L_b / 2)$, where C_D is the drag coefficient, ρ is the density of water, V is the current velocity and A_b and A_f are the projected areas of one boom unit and a fin to the normal velocity component respectively, gives the moment by the boom itself and the moment by all the fins.

The boom moment M_b , as shown in Equation 1 is always positive for reducing the boom angle θ and is independent of the fin angle α . The fin moment M_f , it can be seen from Equation 2 and with reference to Figure 2, consists of two parts. The first part is for reducing the boom angle θ when $\alpha < 90^\circ$ (counterclockwise moment) and increasing θ when $\alpha > 90^\circ$ (clockwise moment), while the second part is always for increasing the boom angle θ (clockwise moment). Since the ice oil boom is for barring ice floes, it should be made to swing into the current as much as possible. The fin angle of the boom α under working conditions, therefore, should be greater than 90° .

When $\alpha > 90^\circ$, it can be seen from Equation 2 that the moment for increasing θ increases with L_a/L_b . Therefore, to obtain the maximum clockwise moment, L_a/L_b should be assigned the maximum value of unity. To make L_a/L_b equal unity, the hinging point of the fin must be placed at the end of the unit.

When the boom is in equilibrium, Equations 1 and 2 are equal and under the conditions of $L_a/L_b = 1$, one has

$$\theta = \cos^{-1} \left\{ \frac{1}{C_D} \left[\frac{L_b \left(\frac{1}{2} \frac{L_b}{L_a} + N \right) + \frac{N^2}{2}}{\frac{L_b}{L_a} + \frac{L_b}{L_a} + \frac{N-1}{2}} \right] \right\} \cos \alpha$$

Equation 3 contains five parameters: L_u/L_b , L_g/L_b , N , A_f/A_b , and L_f/L_b . The effects of these parameters on the $\alpha - \theta$ curve were studied. From the analysis the following conclusions were drawn:

1. For practical ranges, L_u/L_b has little effect on the $\alpha - \theta$ curve. Therefore, the boom angle is not affected appreciably by the length of the upstream protective length. (The analysis was made with $N = 12$.)
2. The number of units of the boom N also has little effect on the angle of the boom. (The analysis was made with $N = 2 - 20$.)
3. L_g/L_b does not significantly increase the boom angle. Therefore, the gap of the fin is mainly to reduce the turbulence, instead of increasing the moment of the boom.
4. The boom angle is significantly increased by increasing the fin area in water, either by increasing the depth or the length of the fin. Comparatively, however, it is more advantageous to increase the length of the fin rather than the depth for the same area of fin.

Figure 3 shows the $\alpha - \theta$ curves of different L_f/L_b values and con-

stant parametric values of L_u/L_b , N , L_g/L_b , and H_f/H_b (H_f and H_b are the depth of fin and boom in water respectively). It may be noted that the upper part of the curves above the α axis was plotted according to Equation 3 while the lower part of the curves was plotted according to another equation which was derived for the boom being deflected to the right instead of to the left. These two equations were similar except for the signs. For a practical ice oil boom, only the upper part of the curves is of interest.

From the curves, one sees that a boom will be in the direction of the flow when the fins are completely open at 180° . As the fins are gradually closed, the boom begins to swing into the flow until a maximum angle is reached. Thereafter, further closing the fins will reduce the boom angle until $\theta = 0$. From that point on, the boom will swing to the other side. It is interesting to see from the curves that the boom then can swing either to a maximum angle before swinging back or continue swinging until the boom points, theoretically, upstream. Such a position, of course, would not really occur because it repre-

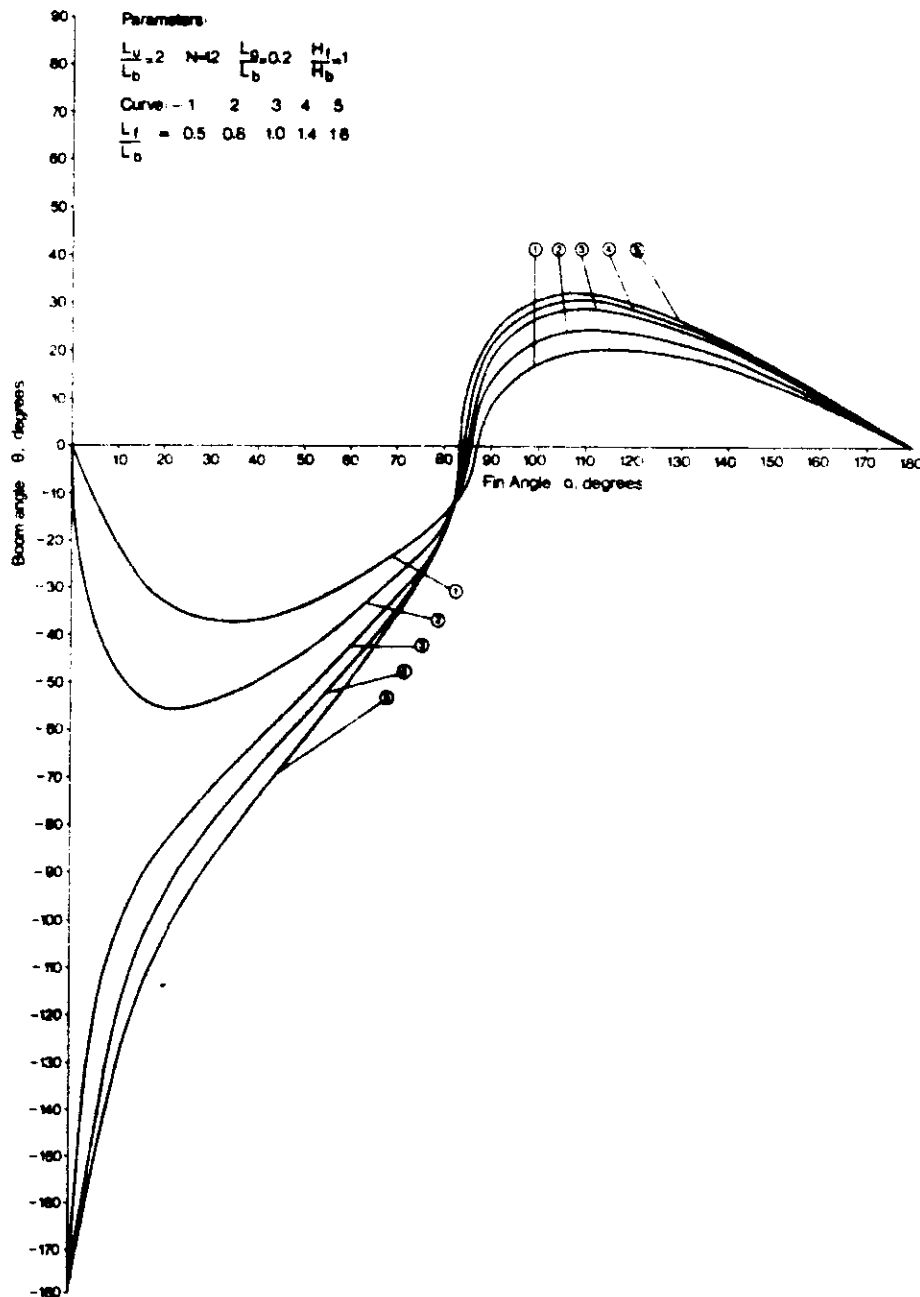


Figure 3. Boom angle and fin angle relationship at different fin lengths

sents the position of unstable equilibrium such as standing a needle on its end. With the slightest disturbance, the boom would suddenly swing downstream.

The parameters chosen in plotting Figure 3 were thought to be reasonable from the engineering point of view. Therefore, a 30° boom angle may be expected of a prototype boom.

From Figure 3 and the above discussions, one sees that the ice oil boom should be initially deployed with its fins open. Then, it can be brought into the current by gradually closing the fin until the maximum boom angle is reached. The nearly linear curve of the $\theta - \sigma$ curves at high fin angles means that the swinging of the boom into the current is almost proportional to the change of the fin angle. Such a characteristic, of course, would make the operation of the boom much easier. From the curves, one also sees that they are quite flat near the θ_{max} point. This means that θ_{max} is insensitive to the fin angle around the optimal fin angle σ_{max} . For field operation of a boom where strict operational control is difficult, such a relaxed operational requirement is very desirable.

A boom should be deployed at optimal fin angle σ_{max} which gives the maximum boom angle θ_{max} . When such a boom is offset by the impact of an ice floe, there will be a reduction of the moment caused by the drag on the boom itself and an increase of the moment caused by the drag on the fins. From theoretical analysis, the non-dimensional reduction of the boom moment is given by

$$\Delta M_{b_0} = \left[\frac{L_u}{L_b} \left(\frac{1}{2} \frac{L_u}{L_b} + N \right) + \frac{N^2}{2} \right] (\sin^2 \theta - \sin^2 \theta_{max}) \quad (4)$$

where θ is the boom angle at the offset position and ΔM_{b_0} is normalized on the same basis as M_{b_0} and M_{f_1} . The non-dimensional increase of the fin moment is given by

$$\Delta M_{f_1} = \frac{1}{2} \left[\frac{A_f}{A_b} N \left(\frac{L_u}{L_b} + \frac{N+1}{2} \right) \cos \sigma_{max} - \frac{A_f}{A_b} N \left(\frac{L_u}{L_b} + \frac{L_f}{2L_b} \right) \right] \cos(2\sigma_{max} + 2\theta_{max}) [1 - \cos 2\Delta\theta - \tan(2\sigma_{max} + 2\theta_{max}) \sin 2\Delta\theta] \quad (5)$$

where $\Delta\theta = \theta_{max} - \theta$.

By equating the normal kinetic energy of the ice floe to the boom to the work overcoming the above two unbalanced moments, one obtains the following equation relating the non-dimensional size of the ice floe V_{i_0} deflected and the yield angle $\Delta\theta$ of the boom.

$$V_{i_0} = \frac{1}{k} \frac{A_i t_i}{L_b^2 H_b} = \frac{\int_{\Delta\theta} (\Delta M_{b_0} + \Delta M_{f_1}) d(\Delta\theta)}{\sin^2(\theta_{max} - \Delta\theta)} \quad (6)$$

where A_i and t_i are the area and thickness of the ice floe respectively, k is a constant affected by the drag coefficient and the shape of the ice floe and should have a value of about unity.

V_{i_0} versus $\Delta\theta$ curves were plotted under different parametric conditions. From the curves, the following conclusions were drawn:

1. For practical ranges, L_u/L_b is not an important parameter in affecting the $V_{i_0} - \Delta\theta$ curve. This means one may not expect to improve the performance of a boom by increasing the gap between the fin and the boom, although this may reduce turbulence.
2. L_u/L_b is also not an important parameter in affecting the $V_{i_0} - \Delta\theta$ curve.
3. Increasing the fin area increases the size of the ice floe that the boom can deflect for a given boom angle. It is more advantageous, however, to increase the length of the fin instead of the depth for the same area of the fin.
4. The ability of a boom in deflecting ice floes increases significantly with the increase of the number of units of the boom.

Figure 4 is a diagram showing the $V_{i_0} - \Delta\theta$ curves of different L_f/L_b values (and reasonable constant values of L_u/L_b , N , H_f/H_b , and L_u/L_b). It can be seen from Figure 4 that the effect of L_f/L_b on the $V_{i_0} - \Delta\theta$ curve is substantial. It is interesting to see, however, that an increased L_f/L_b does not reduce the yield angle $\Delta\theta$ of the boom when hit by an ice floe of given size, but significantly increases the maximum boom angle θ_{max} (where the curve terminates). This results in a large final boom angle θ to shield the ice free area behind the boom.

Figure 5 is a diagram showing the $V_{i_0} - \Delta\theta$ curves of booms of different number of units N . It can be seen from Figure 5 that in this case N does not increase the maximum boom angle θ_{max} , but noticeably moves up the $V_{i_0} - \Delta\theta$ curve. Since the curves are plotted on a vertical logarithmic scale, the ability of the ice oil boom in deflecting ice floes is increased significantly.

The theoretical conclusions reached in this section form the basis for development of the ice oil boom.

Laboratory experiment

Three model boom sections of the shape and dimensions shown in Figure 6 were constructed to verify in the laboratory the theoretical predictions and to obtain the necessary design parameters. The gap between the fin and boom could be adjusted, and the fin angle was variable. Plastic chips and wooden blocks 10 cm x 10 cm x 5 cm (4 in x 4 in x 2 in) were placed in the towing tank before each run to simulate spilled oil and ice floes respectively. For a few runs, large ice sheets measuring 1.2 m x 1.2 m x 2.5 cm (4 ft x 4 ft x 1 in) were used (Figure 7).

The laboratory experiments showed that when being towed with a fin angle of about 90°, the boom as a whole would make an angle of about 40° with the direction of tow. However, the angles made by the three individual boom sections were different. For the upstream section, the angle was the smallest at about 35° and for the last section, the angle was the largest at about 45°. An arch thus was formed by the three sections and the arch hindered the free movement of the simulated ice and oil. The arch was greatly reduced when the second last fin was removed.

Under such a situation, the simulated oil flowed through the openings nicely and the boom smoothly guided the simulated ice blocks to one side. However, when the boom was hit by a large ice pane, it would deform excessively and cause the ice pane to be caught between two boom sections for a time. The total swinging of the boom, as a consequence of being hit by the ice pane, was observed to be small compared to the original boom angle of about 40°. No attempt was made to test the boom with the sections rigidly connected. The tests were repeated at different towing speeds and the speed did not appear to affect the behavior of the boom. For all the experiments, the fin gap width was roughly maintained at $L_u/L_b = 0.25$.

Because of the timing and funding of the program, it was necessary to limit the laboratory testing to preliminary work only, and proceed with the design, construction and field test of a prototype boom.

Field experiment

Based on theoretical investigations and the preliminary laboratory testing, a prototype boom as shown in Figure 8 was designed. The prototype boom was financed and built under contract by the U.S. Coast Guard. The field test was conducted jointly by the Canadian and U.S. Coast Guards, U.S. Army Corps of Engineers, and Environment Canada.

Each boom section consisted of two units of 3.05 m (10 feet) long each; a total of six sections were constructed giving a total boom length of 36.59 m (120 feet). In Figure 8, the dimensions shown on the lines were the design dimensions and the figures shown in brackets were the dimensions of the boom sections as constructed.

Hardwood was inadvertently used to construct the boom instead of the specified cedar. The heavy wood used, plus the construction discrepancy, caused the openings in the boom to be submerged below the water surface. To alleviate the problem, two-inch thick styrofoam slabs were nailed to the bottom of the boom. The styrofoam raised the openings out of the water by about 4 cm (1½ inches) but made the boom unstable and prone to tilting. The stability was greatly improved when the fins were extended out to provide a balance force.

The boom was tested in the Detroit River at the Canadian Coast Guard Depot in Amherstburg, Ontario in March 1978. Figure 9 shows the test site and the experimental layout. The surface velocity of the flow along I-I and II-II was measured with a current meter (Table 1). Because the measurements were made from a boat, a ± 10 percent error range appeared to be reasonable.

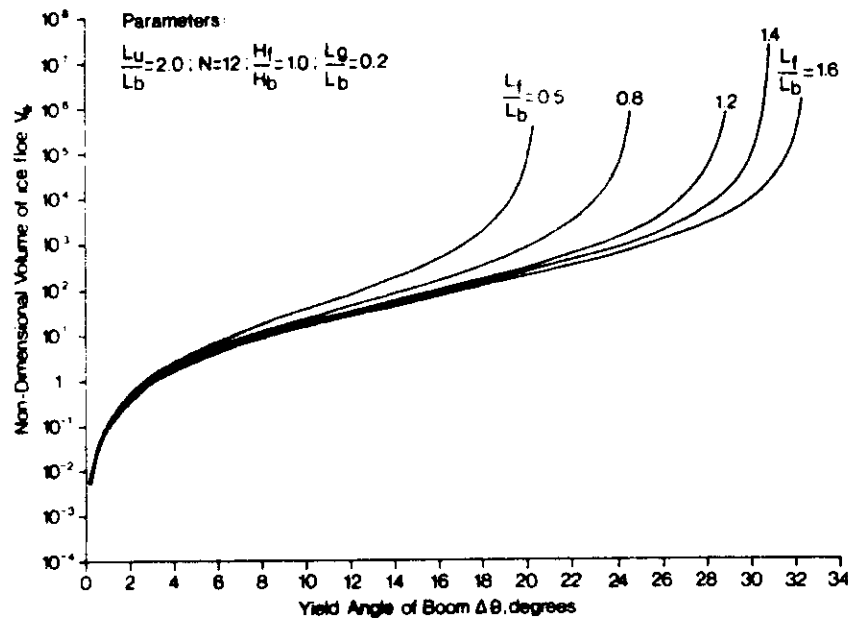


Figure 4. Relationship between size of ice floe and yield angle for booms of different fin lengths

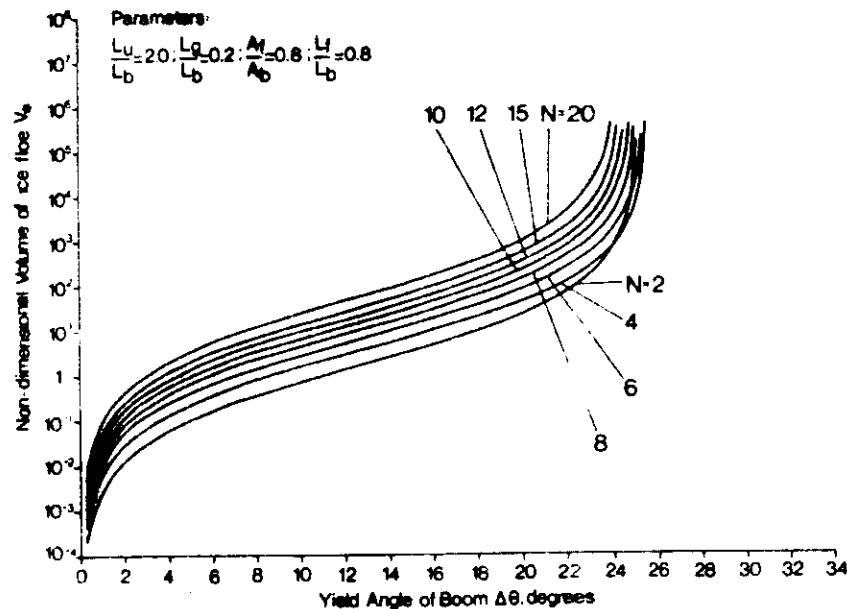


Figure 5. Relationship between size of ice floe and yield angle for booms of different units

Before the exercise, the boom sections and the fins were stacked up beside the bay. With a crew of four and the use of a mobile crane, a section could be fitted with the fins and placed in the water in about 15 minutes; another half an hour was needed to cable the boom section and the fins. With better engineering design and an improved procedure, the deployment time could be greatly reduced. After the boom was assembled, it was towed by tug from the bay into the Detroit River and tied to a bollard on the pier for testing.

Limited testing was first conducted on the flexibly-connected boom. It quickly became evident that a flexible boom would deform excessively when hit by ice floes of relatively large size. The testing, therefore, was concentrated on the rigidly-connected boom. The boom was made rigid by hammering wooden pegs between the boom sections. The boom was very stable under working conditions, even when hit by large ice floes, so the inserting of wooden pegs was done after the boom was deployed.

The fin angles were measured with a protractor by a team member working on the boom. Another team member measured the surface current velocity at the midpoints of each boom section. Two methods were used to measure the boom angles. The first method was to measure the distances from the shore to the upstream and downstream ends of the boom with strings, as simultaneously as practicable, and then calculate the boom angle by trigonometry. The second method was to measure the angles between the baseline and the line of sight to the upstream end and downstream end of the boom from the two survey stations shown in Figure 9 and then calculate the boom angle analytically.

To measure the total force on the boom, both the boom cable and the fin cable were connected to a tension gauge as shown in Figure 9. The fin angle was changed by two men pulling the fin cable by hand.

No attempt was made to record exactly the size of the ice floes and the yielding angles of the boom when it was hit by the ice floes. How-

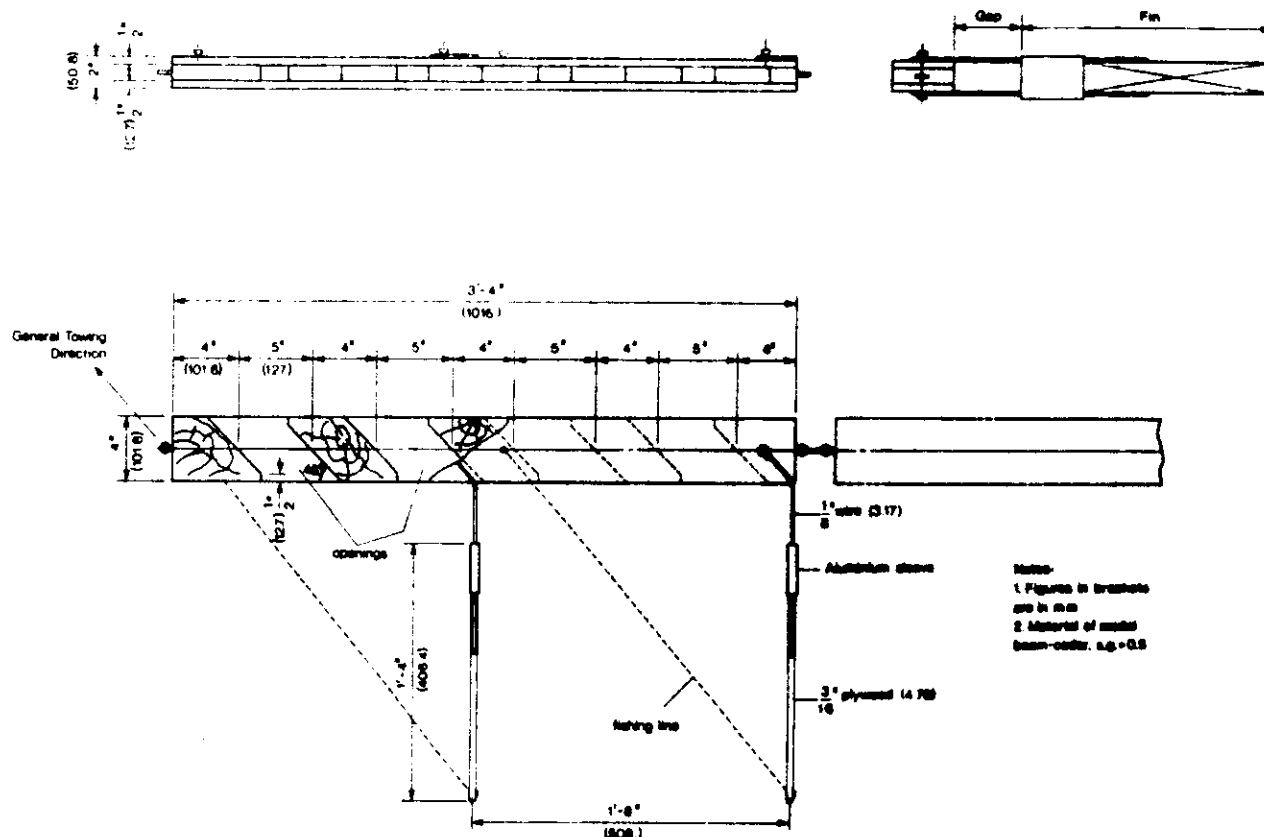


Figure 6. Model boom sections used in laboratory experiments



Figure 7. Laboratory experiment with model boom in towing tank

ever, during the test period when measurements were made, ice floes as large as $20 \text{ m} \times 20 \text{ m} \times 0.2 \text{ m}$ thick ($70 \text{ ft} \times 70 \text{ ft} \times 8 \text{ in}$) by visual estimation were encountered and the measured boom angles should reflect the working of the boom under such conditions.

To study the passing of oil slick through the openings and deflection of oil by the fins to the shore, plastic oil simulant was released upstream of the boom from a tug. Figure 10 contains two pictures showing the oil simulant testing. The upper picture shows the passing of the oil simulant through the openings and the simultaneous deflection of an ice floe by the boom. The lower picture shows the oil simulant being carried toward the shore by the surface current as deflected by the fins. Observations showed that only the oil simulant caught between ice floes could not pass through the openings. This was remarkable considering that the openings were not properly positioned due to construction errors. The observations also showed that the deflected current had no problem in carrying the oil simulant over more than 30 m (100 ft) to the shore.

A total of 14 tests were conducted; the experimental results are tabulated in Table 2. From the table one can see that the presence of the boom in the flow did not significantly reduce the flow velocity, although it might have changed its direction. (The velocity was measured with a Price current meter which is nondirectional.)

From Table 2 one also sees that the connection of all fins by a single cable allowed an accumulated error of the fin angle to arise. For the tested range of fin angles, more than 10° difference in fin angle between different fins was not uncommon. This suggested that either the fins should be maneuvered individually, or only a few of them should be connected and maneuvered as a group.

The boom angles measured with theodolites and the boom angles measured with string lengths under similar conditions were quite close, as shown in Table 2. This means that in future studies, either way may be used depending on experimental particulars.

According to Table 2, the boom angle θ was plotted against the fin angle α for the tested boom as shown in Figure 11. In Figure 11, the

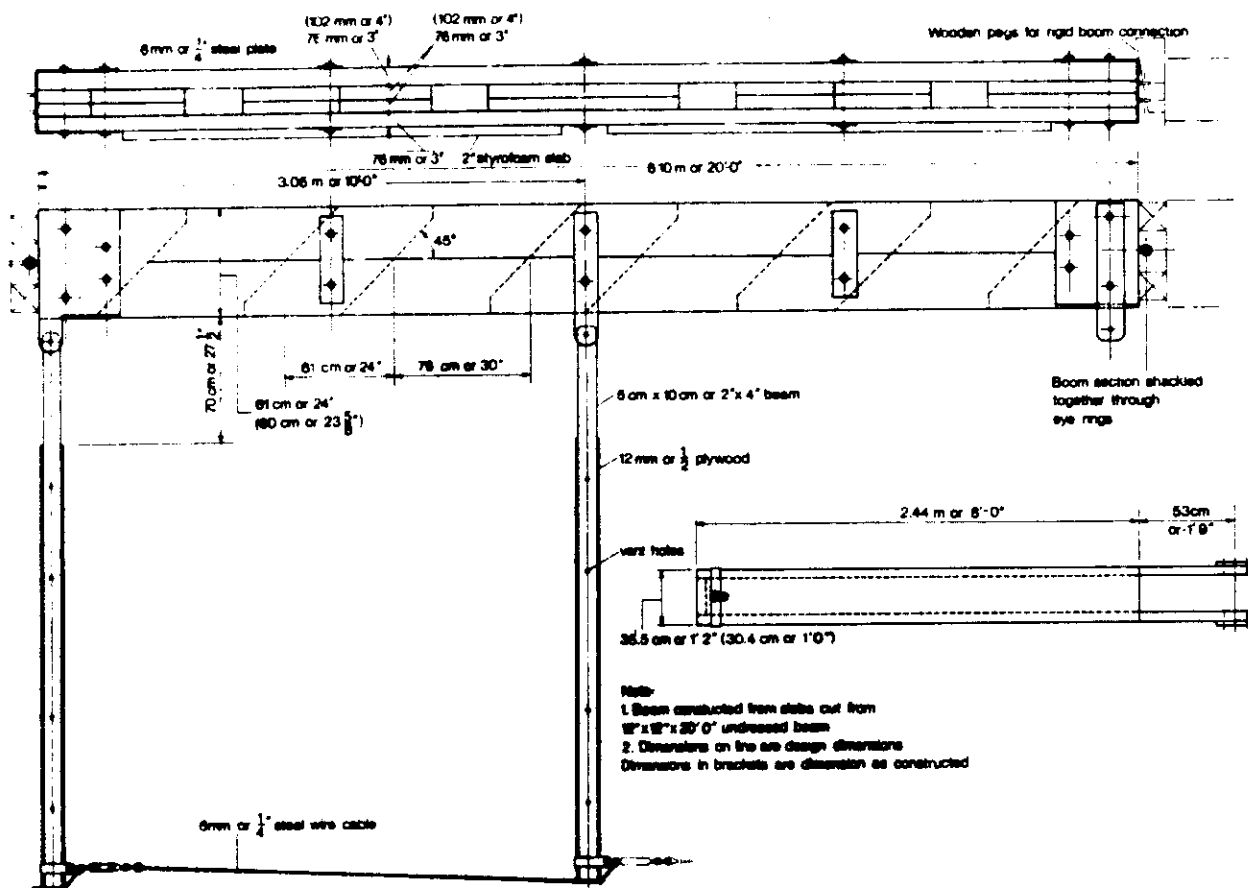


Figure 8. Prototype boom for field test

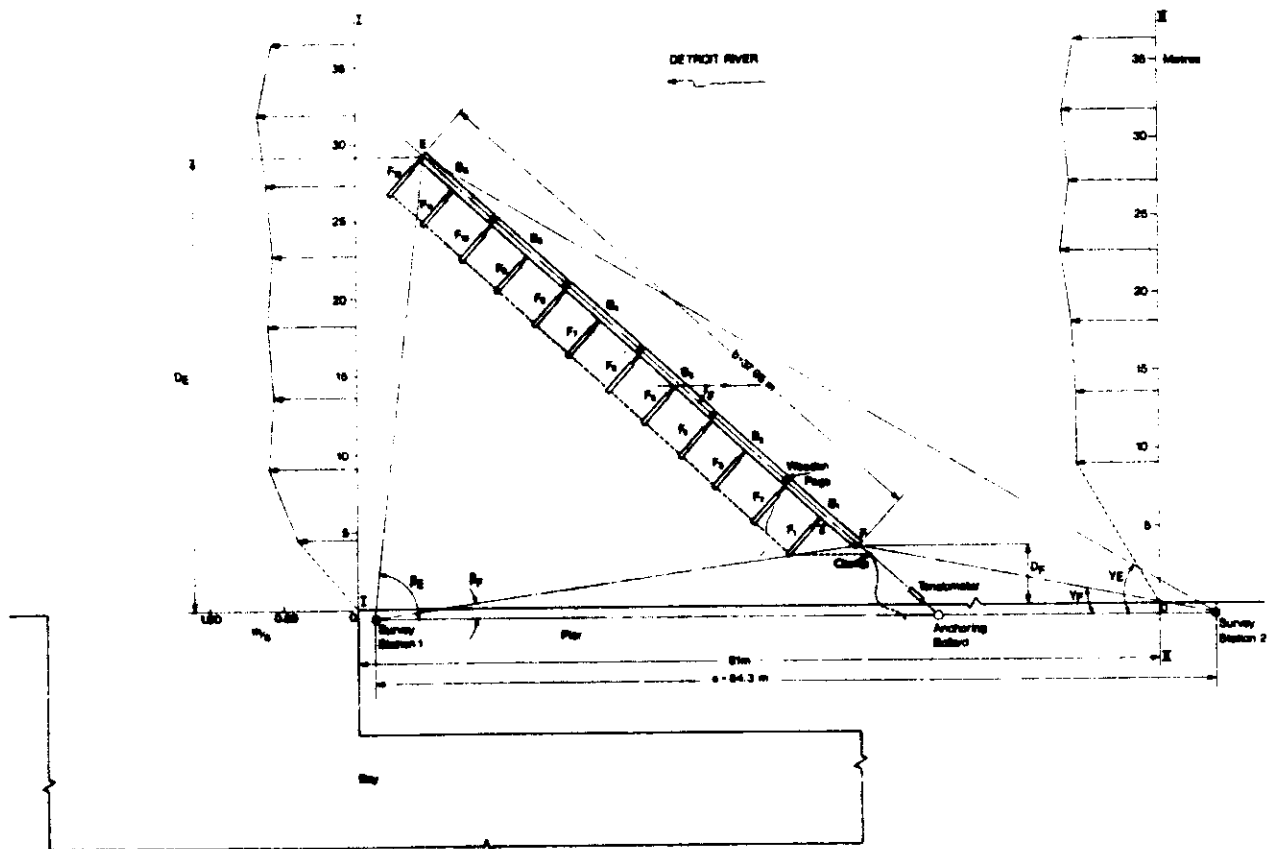


Figure 9. Experimental layout for field testing of ice-oil boom

Table 1. Surface velocity of current at test site

Distance from shore		Velocity along I-I		Velocity along II-II	
m	ft	m/sec	ft/sec	m/sec	ft/sec
4.57	15.0	0.40	1.3	—	—
9.15	30.0	0.58	1.9	0.55	1.8
13.72	45.0	0.55	1.8	0.55	1.8
18.29	60.0	0.58	1.9	0.58	1.9
22.87	75.0	0.55	1.8	0.64	2.1
27.44	90.0	0.58	1.9	0.58	1.9
32.01	105.0	0.64	2.1	0.64	2.1
36.59	120.0	0.55	1.8	0.55	1.8

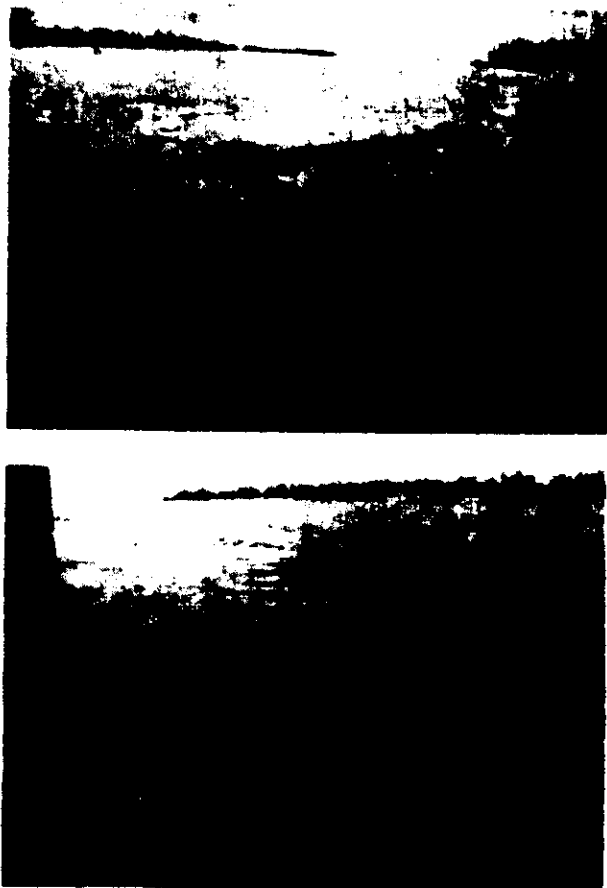
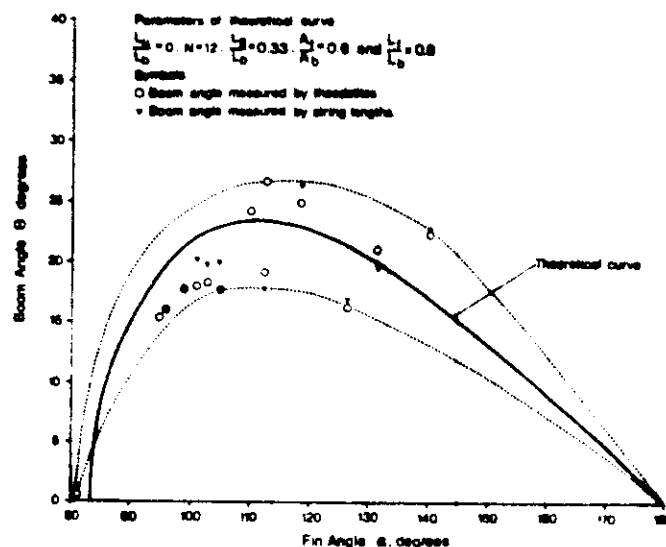


Figure 10. Field experiment with prototype boom

theoretical $\theta - \sigma$ curve for the prototype boom was also plotted. The parameters of the prototype boom, based on the actual construction dimensions, were $L_u/L_b = 0$, $N = 12$, $L_f/L_b = 0.33$, $A_f/A_b = 0.6$, and $L_r/L_b = 0.8$. In Figure 11, two enveloping curves containing the data points were also drawn.

From Figure 11 one can see that within the reasonably expected experimental error range, the field experiment supported the theoretical predictions. The data points scatter closely about the theoretical curve and the two enveloping curves are of similar shape to the theoretical curve.

Should everything come nicely together, the upper enveloping curve should be more or less coincident with the theoretical curve. However, this is not the case and from Figure 11 one sees that the upper enveloping curve in places is up to 5° above the theoretical curve. The θ_{\max} values of the two curves are different by about 3.5° . Two things could have caused this. The first was that because of the tilting of the boom as a consequence of nailing styrofoam to the bottom of the boom, the fins were immersed in water more than if the boom floated squarely on the water. A greater drag, therefore, was exerted on the fins than

Figure 11. Comparison of $\theta - \sigma$ relationship between experimental results and theoretical predictions

otherwise would have been, causing the boom to swing more into the flow. The second reason was that because the openings in the boom were chambered, the flow through them would have met less resistance than when it encountered the fins. In other words, the drag coefficient for the boom body should be less than that for the fins. A greater drag coefficient for the fins than for the boom means that the boom would swing more into the flow.

Considering the upper enveloping curve approximately as the ice free curve of the prototype boom, from Figure 11 one sees that the maximum yield angle of the boom during the experiment was about 9.5° . Presumably this maximum yield angle took place when the boom was hit by the largest ice floe of $20 \text{ m} \times 20 \text{ m} \times 0.2 \text{ m}$.

The theoretical relationship between the yield angle and the floe size for the prototype boom was calculated and plotted as shown in Figure 12. It can be seen from Figure 11 that with a yield angle of 9.5° the non-dimensional size of the ice floe that may be deflected is $V_{L_0} = 17$.

Knowing V_{L_0} , the area of the ice floe can be calculated from the definition of V_{L_0} (see Equation 6). Using the values of $k = 1$, $t_f = 20 \text{ cm}$, $H_b = 23 \text{ cm}$ and $L_b = 3.05 \text{ m}$, a floe size of $13.5 \text{ m} \times 13.5 \text{ m} \times 0.2 \text{ m}$ is calculated, which is comparable to the largest observed floe size of $20 \text{ m} \times 20 \text{ m} \times 0.2 \text{ m}$ estimated visually.

Although an effort was made to measure the drag on the boom, unfortunately, the tensionmeter malfunctioned. However, it was found that three men together could pull the boom and two men could adjust the fin angles.

Conclusions

Based on the theoretical analysis and the field experiment, it was demonstrated that an ice oil boom can be built for satisfactory deployment on flowing water infested with ice floes to enable oil spill containment and recovery.

Further work is being conducted both in the laboratory and in the field to improve the design and performance of the ice oil boom. The results of the investigation will be reported upon completion.

Acknowledgment

This project would not have been possible without the cooperation and support received from many individuals and organizations. Special gratitude is due to Cdr. C. Corbett, USCG, who managed the contract for the prototype boom; to Capt. J. Bennett, CCG, who su-

Table 2. Results of field experiment

Test No.	Fin Angle α , degrees												Surface Velocity of Current V^* , m/sec							Boom Angle θ , degrees		
	f_1	f_2	f_3	f_4	f_5	f_6	f_7	f_8	f_9	f_{10}	f_{11}	f_{12}	Avg	B_1	B_2	B_3	B_4	B_5	B_6	Avg	B_y Survey	By string lengths msmt.
1	78**	78**	76	76	76	78	81	81	82	85	88	90	81.3	0.46	0.58	0.58	0.46	0.43	0.46	0.49	0.5	—
2	—	—	92	93	92	92	97	96	101	93	96	96	94.8	0.36	0.37	0.52	0.58	0.64	0.55	0.50	15.4	—
3	105	106	109	111	111	112	116	117	113	112	119	120	112.5	0.40	0.43	0.55	0.46	0.46	0.58	0.48	26.5	—
4	107	107	111	111	111	111	113	110	109	109	107	114	110.0	0.43	0.67	0.58	0.58	0.46	0.58	0.54	24.3	—
5	89	91	92	93	96	96	99	99	98	98	100	100	95.9	0.27	0.46	0.43	0.52	0.58	0.52	0.46	16.0	16.1
6	92	92	96	97	99	99	102	102	102	101	102	102	98.8	0.46	0.43	0.64	0.64	0.58	0.64	0.56	17.8	17.6
7	101	101	101	99	101	101	101	101	101	100	103	102	101.0	0.46	0.52	0.58	0.67	0.64	0.64	0.59	18.0	20.1
8	96	96	101	102	102	104	105	105	104	104	104	106	102.6	0.46	0.52	0.55	0.55	0.64	0.64	0.56	18.3	19.7
9	99	101	103	103	105	105	108	107	106	106	108	107	104.8	0.40	0.46	0.55	0.58	0.64	0.58	0.53	17.8	19.8*, 17.6*
10	109	109	111	111	111	111	115	115	112	112	115	115	112.2	0.52	0.43	0.58	0.58	0.58	0.67	0.56	19.1	17.7
11	116	118	120	118	118	118	120	118	118	118	118	118	118.2	0.40	0.55	0.52	0.67	0.64	0.64	0.57	25.0	26.4
12	127	127	127	127	127	127	128	128	125	124	124	125	126.3	0.46	0.58	0.52	0.46	0.55	0.58	0.52	16.1	16.9
13	134	—	132	—	132	—	134	—	128	—	127	—	131.2	0.46	0.52	0.52	0.43	0.64	0.64	0.53	21.1	19.6
14	—	148	147	146	144	141	141	140	134	133	134	133	140.0	0.52	0.52	0.46	0.43	0.58	0.58	0.52	22.4	22.7

- Notes: 1. See Figure 9 for order of boom sections and fins
 2. Velocity was measured at midpoint of boom section
 3. Boom angle by string length measurement is calculated from $\sin \theta = (D_E - D_F)/b$ (Figure 9)
 4. Boom angle by survey was calculated from (Figure 9)

$$\sin \theta = \frac{a}{b} \frac{\sin \beta_E \sin \gamma_E}{\sin (\beta_E + \gamma_E)} - \frac{\sin \beta_F \sin \gamma_F}{\sin (\beta_F + \gamma_F)}$$

5. During the experiment, the wind was from the south-southwest at seven knots; ice was in the form of low density ice floes (i.e., as discrete floes)
 6. Thickness of ice: large floes—15-20 cm; small floes—8-10 cm; occasionally 30 cm
 * Under different ice conditions
 ** Fins touching shore

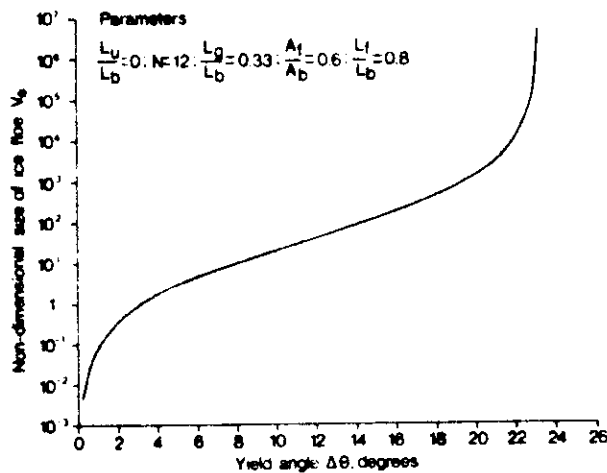


Figure 12. Theoretical relationship between deflected floe size and yield angle for the prototype boom

pervised the field test; to Capt. C. Beckett, CCG, who assisted in organizing the field program; and to Y. L. Lau who reviewed the report.

References

1. Brodsky, L., M. E. Charles, G. D. Greene, and D. Mackay, 1977. The Use of Deflectors for the Deployment of Oil Booms at an Angle to River Currents. PACE report No. 77-3. Petroleum Association for Conservation of the Canadian Environment
2. Eryuzlu, N. E. and R. Hausser, 1977. Use of floating deflector for oil spill control in fast flowing waters. *Proceedings of the 1977 Oil Spill Conference*. American Petroleum Institute, Washington, D.C. pp335-340
3. Foley, J. P. and S. J. Tressidder, 1977. The St. Lawrence River oil spill of June 23, 1976—Are you ever truly ready. *Proceedings of the 1977 Oil Spill Conference*. American Petroleum Institute, Washington, D.C. pp81-86
4. Tsang, G., 1975. Ice Conditions and the Proposed Containment and Removal of Spilled Oil on the St. Clair and Detroit Rivers. Scientific Series No. 56. Inland Waters Directorate, Environment Canada
5. Tsang, G. and N. Vanderkooy, 1979. Theory, Development and Testing of an Ice-Oil Boom for Flowing Water. Environmental Protection Service report. (in press)
6. Vanderkooy, N., A. Robertson, and C. J. Beckett, 1976. Evaluation of Oil Spill Barriers and Deployment Techniques for the St. Clair-Detroit River System. Technology Development Report, EPS-4-EC-76-r. Environmental Protection Service, Environment Canada